Neutrinos from the gamma-ray source eHWC J1825-134: Predictions for Km^3 detectors

V. Niro,[1,*] A. Neronov,[1,2,†] L. Fusco,[1,‡] S. Gabici,[1,§] and D. Semikoz[1,¶]

Université de Paris, CNRS, Astroparticule et Cosmologie, F-75006 Paris, France
Astronomy Department, University of Geneva, Chemin d'Ecogia 16, 1290 Versoix, Switzerland

(Received 19 April 2021; accepted 9 June 2021; published 15 July 2021)

The eHWC J1825-134 source is located in the southern sky and has been recently detected by the HAWC observatory. It presents an hard spectral index and its gamma-ray flux extends up to energies close to 100 TeV without significant suppression. Amongst the HAWC sources, it is the most luminous in the multi-TeV domain and therefore is one of the first that should be searched for with a neutrino telescope in the northern hemisphere. Using an updated effective area for the forthcoming KM3NeT detector, we study the possibility to detect this source within ten years of its running time. We show how the *Fermi*-LAT data could help in providing a morphology information on the source region. We conclude that, considering a neutrino energy threshold around 10 TeV, about a four to five sigma detection has to be expected after ten years of observations, depending on the details of the considered scenario. Finally, we also consider the case in which the emission from the HWC J1825-134 source is only partially hadronic and show that in 20 years of running time a three sigma detection is feasible.

DOI: 10.1103/PhysRevD.104.023017

I. INTRODUCTION

The observed energy spectrum of cosmic rays is described by a power law with spectral index of about 2.7 up to energies of a few PeV, where the spectrum gets steeper and a feature called the "knee" originates [1,2]. The knee is believed to mark the maximum energy for cosmic rays accelerated at Galactic sources [3], or alternatively the energy above which the effectiveness of the confinement within the Galaxy is reduced [4].

The problem of the origin of galactic cosmic rays is one of the most important problems in high energy astrophysics [1,2]. This is particularly true for energies around the knee or greater, since explaining the origin of cosmic rays in that energy range is problematic [5]. Different possible sources of galactic cosmic rays have been proposed, among which supernova remnants, proposed in 1934 by Baade and Zwicky, are the most accredited ones [6]. It is, however, not clear whether supernova remnants can accelerate cosmic rays up to PeV energies or if other sources should be considered. With this respect, we recall that evidence for the acceleration of PeV particles in the Galactic center has been reported by the H.E.S.S. Collaboration [7].

During the acceleration of cosmic rays, the production of gamma rays is expected. These could be produced from the decay of neutral pions, arising from the hadronic interactions with the interstellar medium, or from leptonic processes, like inverse compton, that is however suppressed by the Klein-Nishina effect in the multi-TeV energy domain [8]. The identification of the origin of the gamma-ray emission, specifically if it is leptonic or hadronic is thus one of the most important goals in gamma-ray astronomy.

If cosmic rays lose part of their energy in hadronic processes, then, a flux of high energy neutrinos is expected from charged pion decays. Neutrino telescopes are, for this reason, able to provide important information on the production mechanisms of cosmic rays as the detection of neutrinos from a gamma-ray source would imply that the emission is hadronic.

From the data collected in 7.5 years of running of the IceCube detector, 102 neutrino events were identified (high-energy starting events), including 60 events with deposited energy $E_{\rm dep} > 60$ TeV [9].

At present, the event distribution is consistent with isotropy and therefore often interpreted in terms of extragalactic sources (see for example Ref. [10] for a recent review). However, Galactic scenarios have also been proposed (see for example Refs. [11,12] on this topic). On the galactic and extragalactic contributions of the flux see also the analyses in Refs. [13–18]. Moreover, at the moment a 3.5σ evidence is present for neutrino emission coming from the direction of the blazar TXS $0506+056$ (see Refs. [19–23]).

A multi-messenger search is mandatory for the identification of the origin of cosmic neutrinos. Indeed, gamma-ray

*viviana.niro@apc.in2p3.fr
†andrii.neronov@apc.in2p3.fr
‡luigi.fusco@apc.in2p3.fr
§gabici@apc.in2p3.fr
¶semikoz@apc.in2p3.fr

TABLE I. Extension of the source in degrees, flux ϕ_0 in units of 10^{-13} TeV^{-1} cm^{-2} s^{-1}, spectral index α_γ and cut off energy $E_{\mathrm{cut},\gamma}$.

Source	σ_{ext}	ϕ_0	α_γ	$E_{\mathrm{cut},\gamma}$
eHWC J1825-134	0.53 ± 0.02	2.12 ± 0.15	2.12 ± 0.06	61 ± 12

data are necessary to make correct estimations of neutrino fluxes from point sources. The characteristic gamma-ray feature of a PeVatron include a hadronic, hard spectrum that extends until at least several tens of TeV. To search for these PeVatrons a gamma-ray experiment with detection sensitivity up to about 100 TeV is of fundamental importance.

The High Altitude Water Cherenkov (HAWC) observatory is a gamma-ray observatory sensitive in the multi-TeV energy domain. For this reason, it is currently the most sensitive gamma-ray detector for discovering PeVatrons. The HAWC observatory has reported new data on galactic sources in recent years (see e.g., [24–26]). Among these sources, the eHWC J1825-134 source, located in the southern sky, has been detected with an hard spectrum that extends up to multi-TeV energies, thus it represents a possible PeVatron source. Moreover, this is the brightest source detected by HAWC in the multi-TeV domain.

Note that the IceCube detector has an optimal sensitivity for sources located in the northern hemisphere, and is less sensitive to sources located in the southern sky, using tracks events. For sources in the Southgern sky the sensitivity is roughly an order of magnitude less sensitive if one considers only track events and a spectrum of the type $dN/dE \propto E^{-2}$, while more than two orders of magnitude for a source $dN/dE \propto E^{-3}$, see Fig. 3 in Ref. [27]. The use of cascade events, arising from neutrinos of all flavors, and of the DeepCore subarrays improve the sensitivity of IceCube to the sources in the southern celestial hemisphere, compared to the use of only tracks events [27]. For a search of several TeV gamma-ray sources observed by HESS in the southern sky with IceCube we refer to Ref. [28]. A kilometer-cube detector in the northern hemisphere, instead, will see these events as muon events, for which a good angular reconstruction is possible and could use all its volume for the point sources analysis. The importance of a kilometer-cube detector in the northern hemisphere was pointed out considering numerous galactic sources in Ref. [29]. Moreover, it was also previously considered in connection with the prospects of detecting young supernova remnants [30,31] and the Milagro diffuse flux from the inner galaxy [32].

Several studies have been carried out about the possible detection of Galactic sources in the northern hemisphere at IceCube, in particular considering sources detected by the Milagro Collaboration (see e.g., [33–35]). It was found that for specific sources, a discovery at three standard deviations in less than 10 years is feasible [36,37]. However, the predictions are affected by the discrepancies between information coming from different gamma-ray experiments, air-Cherenkov telescopes, and air-shower detectors, probably due to the different field of view and energy range. For a recent update, about the Milagro sources and considering the new HAWC data, we refer to Ref. [38].

In this work we present modeling of the source eHWC J1825-134. In Sec. II, we describe the data present in the literature on the source, while in Sec. III, the calculation of the neutrino flux and the KM3NeT/ARCA effective area is considered. In Sec. IV, we present our results, and in Sec. V we present our conclusions.

II. THE EHWC J1825-134 SOURCE

As motivated in the introduction, in this work we will consider the source eHWC J1825-134, analyzed in Ref. [26]. This source is located in the southern sky with a right ascension of 276.40° and a declination of −13.37°. We will use for the analysis the spectrum reported in Ref. [26], where a power law with exponential cut off fit was considered

$$\frac{dN_\gamma}{dE_\gamma} = \phi_0 \left(\frac{E_\gamma}{10\ \mathrm{TeV}}\right)^{-\alpha_\gamma} \exp\left(-\frac{E_\gamma}{E_{\mathrm{cut},\gamma}}\right), \qquad (1)$$

with $E_{\mathrm{cut},\gamma}$ being the cut off energy of the gamma-ray spectrum, α_γ the spectral index and ϕ_0 the flux normalized, (see values in Table I). The sensitivity of HAWC to the high energy tail of the spectrum is of fundamental importance for the correct prediction of the neutrino flux. Note that the flux provided by HAWC for this source at 10 TeV is higher than the one reported by the same collaboration for the Crab nebulae [39,40]—that is about 10^{-13} TeV^{-1} cm^{-2} s^{-1} considering the one sigma systematic error. Thus, this source is one of the brightest sources in the sky and one of the first that should be considered in the analysis of neutrino flux for the KM3NeT detector.

Finally, it should be noted that the region under examination is quite complex. First of all, as pointed out in [26], eHWC J1825-134 overlaps with two HESS sources: the very bright HESS J1825-137 [41,42] and the much weaker HESS J1826-130 [43]. Second, as we will show in Sec. IV, *Fermi*-LAT data reveal the presence of an extended emission in the region.

III. THE NEUTRINO FLUX AND THE KM3NET/ARCA EFFECTIVE AREA

In this work we will consider the possible detection of the source eHWC J1825-134 at the KM3NeT detector

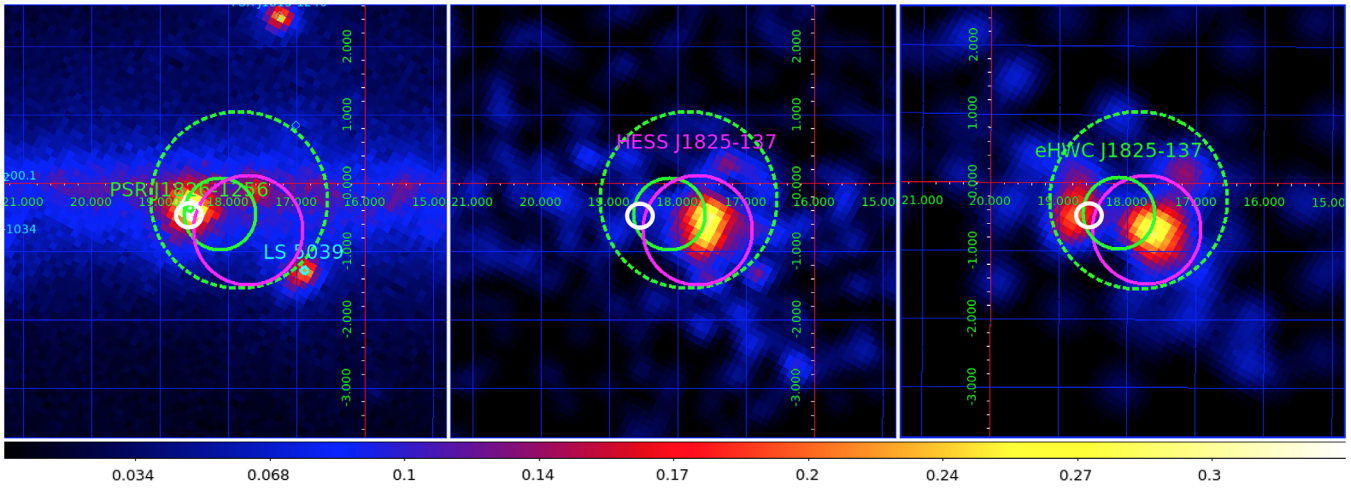

FIG. 1. *Fermi*-LAT countmaps of the source region in 1-10, 100-300 and >300 GeV energy ranges (left to right). The 1–10 GeV and 100–300 GeV maps are smoothed with 0.3 degree Gaussian, the 300 GeV map is smoothed with 0.5 degree Gaussian. The white circle marks the position of HESS J1826-130. The magenta circle is for HESS J1825-137, the green solid circle is for eHWC 1825-134. The dashed circles encode the 1 TeV emission as observed by *Fermi*-LAT.

through tracks events originated by muon neutrino charged current interactions. In particular, we will make the assumption that the gamma-ray emission from the source is fully hadronic, and thus neutrinos result from the decay of charged pions, muons, and kaons [44]. Moreover, we make the assumption that gamma-rays are not absorbed, which is very reasonable for an extended source, and thus our calculation should be considered as a lower bound on the number of neutrinos expected.

In this section, we report the calculation for the neutrino events, using the KM3NeT effective area. Note that the effective area for muon neutrinos has to be corrected by the background rejection efficiency, in order to account for the loss in events due to event selections. In order to obtain an approximate value for this procedure, we considered the letter of intent of the KM3NeT collaboration which contains the expected performance of the KM3NeT/ARCA detector [45]. For this specific case, we will consider the selection cut in the parameter Λ reported there, which gives an effective area optimized for energies above 1 TeV. The total effective area, the selection efficiency, and the effective area optimized for energies above 1 TeV are reported in the left panel of Fig. 3.

The event rate at KM3NeT can be described by the expression reported in Ref. [46]

$$N_{\rm ev} = \epsilon_\theta \epsilon_v t \int_{E_\nu^{\rm th}} dE_\nu \frac{dN_\nu(E_\nu)}{dE_\nu} \times A_\nu^{\rm eff}, \qquad (2)$$

where a sum over neutrino and antineutrino contributions is implicit. The parameter $\epsilon_v = 0.57$ is the visibility of the source (fraction of time when the source is below the horizon), while $\epsilon_\theta = 0.72$ takes into account a reduction factor due to the fact that only a fraction of the signal will be detected if the source morphology is assumed to be a Gaussian of standard deviation $\sigma_{\rm ext}$ and the signal is extracted within a circular region of radius $\sigma_{\rm eff} = 1.6\sqrt{\sigma_{\rm ext}^2 + \sigma_{\rm res}^2}$ [47]. Here, $\sigma_{\rm res} \sim 0.1°$ is the angular resolution of KM3NeT/ARCA [45]. The number of neutrino events $\frac{dN_\nu(E_\nu)}{dE_\nu}$ has been calculated starting from the gamma-ray spectrum and considering the expressions given in Ref. [44] (see also Ref. [48] for another derivation).

The expected atmospheric muon neutrinos are calculated as described in Ref. [36], using Refs. [49–51]. The flux is then integrated over an opening angle equal to $\Omega = \pi\sigma_{\rm eff}^2$.

IV. RESULTS

A. *Fermi*-LAT observations

Before proceeding with the estimate of the expected neutrino flux, we report in Figs. 1 and 2 the results of our analysis of the region using *Fermi*-LAT data. For this analysis we have used events of the SOURCEVETO class which are characterized by low residual cosmic ray background contamination [52,53]. We have filtered the events collected within time interval 246758401 s < MET < 582686231 s using the *gtselect-gtmktime* sequence as described in *Fermi*-LAT analysis threads.[1] Figure 1 shows the count maps of the source region in different energy ranges. The left panel shows the 1–10 GeV map smoothed with 0.3 degree Gaussian. The dominant source in the region is the pulsar PSR J1826-1256. The HAWC source (green solid circle) is immediately adjacent to the pulsar location. The pulsar is not visible in the energy range

[1] https://fermi.gsfc.nasa.gov/ssc/data/analysis/scitools/

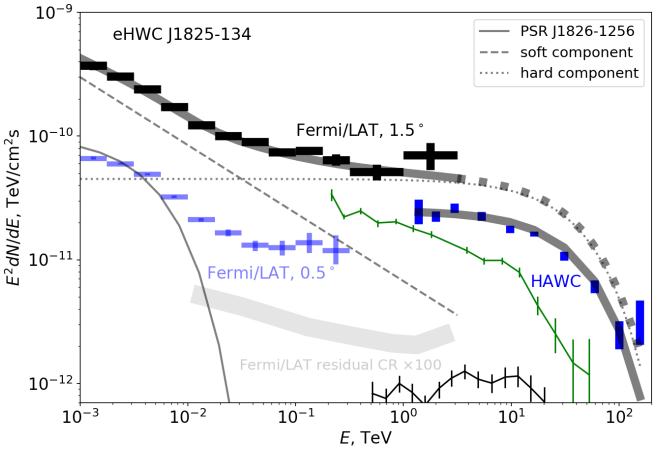

FIG. 2. Spectrum of eHWC J1825-134 region measured by *Fermi*-LAT compared to the HAWC and HESS spectral measurements. Blue thin data points show the spectrum extracted from a circular region of the radius 0.5° around the source position of the HAWC source. Black thick data points are for the spectrum extracted from the 1.5° radius region shown in the right panel of Fig. 1. Dashed, dotted and thin solid curves show spectral fit components. The hard component (dotted line) shape is adjusted to fit HAWC data above 1 TeV. Its normalization is found from the fit to the *Fermi*-LAT data. Green thin data points show the spectrum for HESS J1825-137 and black thin data point the spectrum for HESS J1826-130. The shaded gray band represents the *Fermi*-LAT residual CR background rescaled by hundred.

above 100 GeV, as one could see from the middle panel of Fig. 1. In this energy range the centroid of the source is at the position of the extended source HESS J1825-137, identified as a pulsar wind nebula. In the energy range above 300 GeV the source centroid shifts back toward the position of the pulsar. This might explain the mismatch between the source positions measured by HESS and HAWC. One could notice that the *Fermi*-LAT source consists of two components and the position of the HAWC source is in between them. Therefore, given this complicated source morphology, it is not possible to find an exact match between the HAWC extended source and the different source components observed by *Fermi*-LAT.

In Fig. 2 we show the results of the *Fermi*-LAT spectral analysis which is based on the aperture photometry approach.[2] This is a reliable approach given the uncertain morphology of the source. Blue thin data points show the spectrum of the source region extracted from 0.5° radius circle centered at the position of the HAWC source (green solid circle). How does this compare with the flux measured by HAWC?

The total flux of the HAWC source (blue data points in Fig. 2) has been extracted within a large region, under the assumption that the source has a Gaussian morphology. The region containing 68% of the HAWC flux has a radius of $\sigma_{\rm ext} = 0.53$ degrees [26] and is indicated with the green solid circle in Fig. 1. Therefore, one can see that the HAWC flux within $\sigma_{\rm ext}$ is slightly larger than the flux measured by *Fermi*-LAT, but still consistent within the statistical errors. We report in the figure also the data points for HESS J1825-137 considering an opening angle of 0.8° [42] and HESS J1826-130 [42]. The sum of the two sources at 10 TeV is roughly half the flux measured by HAWC. Note, however, that the gamma-ray emission from the PWN can be ascribed to leptonic [54] as well as hadronic models [55–57]. Neutrino telescopes can actually be used to probe these different scenarios and reveal the nature of the gamma-ray emission.

The black data points in Fig. 2 show the source spectrum extracted from the region which encompasses the ∼1 TeV emission as observed by *Fermi*-LAT (the green dashed circle of radius 1.5° in Fig. 1), see also Ref. [58] on this topic. We find that the flux level measured by *Fermi*-LAT in the TeV range is somewhat higher than that of HAWC. Note that the HAWC analysis assumes a Gaussian source morphology convolved with the HAWC point spread function, which does not match the complex morphology seen by *Fermi*-LAT.

The 1.5° region of the HAWC/HESS source includes, apart from the extended source itself, also the pulsar PSR J1826-1256 and the diffuse emission from the Galactic disk in front/behind the HAWC/HESS source. Taking this into account, we model the source spectrum measured by *Fermi*-LAT with three model components. For the PSR J1826-1256, we adopt the spectrum cited in the *Fermi* 4FGL catalog [59]. The spectrum of the diffuse emission from the inner Galactic disk is well modeled with the power law spectrum with the slope $\Gamma \simeq 2.5$ [60,61]. The spectrum shown in Fig. 2 exhibits a high-energy hardening, which could be modeled adding a cut off power law component to the spectral model. Fitting together the sum of the soft power law (Galactic Disk), the hard cut off power law (the HAWC/HESS source), and the pulsar, we find the fit shown in Fig. 2. We find that the normalization of the cut off power law found from the fit is a factor of 1.5 times higher for the *Fermi*-LAT as compared to the HAWC spectral fit. For completeness we also show in Fig. 2, the level of residual cosmic ray background—see Ref. [53] for more details on the topic—that results in much lower spectra than reported by the HAWC Collaboration.

The discrepancy between the *Fermi*-LAT and HAWC fluxes at photon energy around 1 TeV could be possibly ascribed either to the simple source morphology assumed to extract the HAWC flux, or to the difficulty of estimation of the cosmic ray background in the source region [53], or to systematic errors [26]. Given these uncertainties, in the following we estimate the expected number of neutrino events in KM3NeT from the region in two different scenarios. In particular, we will work under the assumption

[2]https://fermi.gsfc.nasa.gov/ssc/data/analysis/scitools/aperture_photometry.html

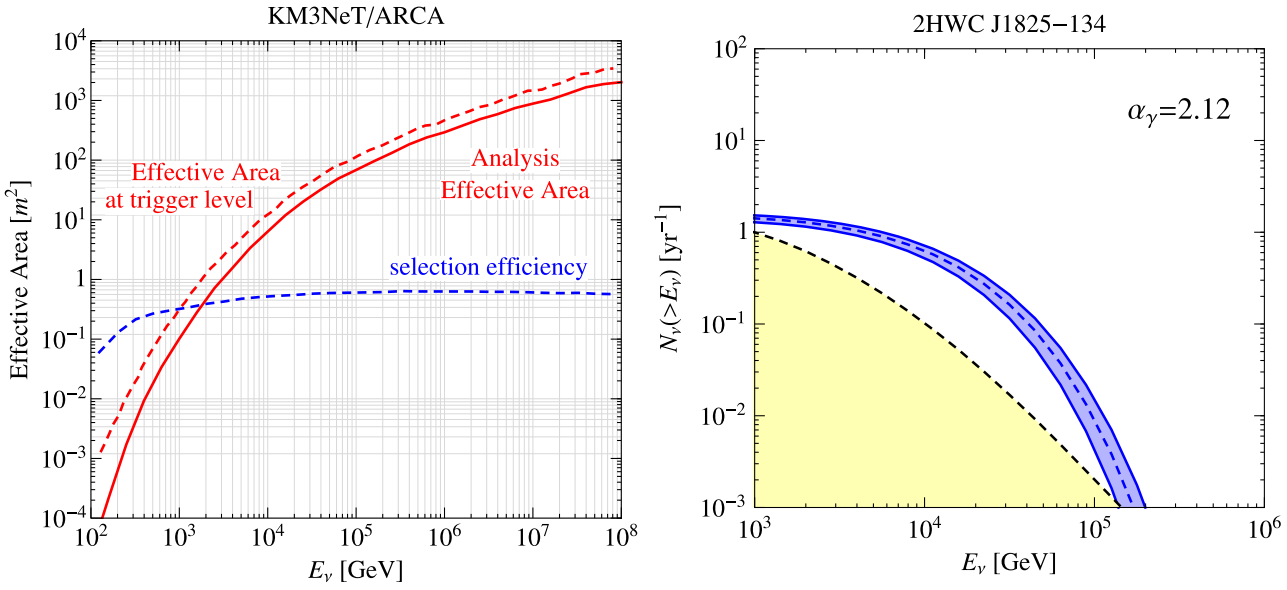

FIG. 3. Left: We show the effective area used in the analysis (red solid line), the effective area at trigger level (red dashed line), and the trigger efficiency (blue dashed), which gives an effective area optimized for energies above 1 TeV; Right: number of events expected for the atmospheric background (yellow area) and for the source for the best-fit value of α_γ and different values of $E_{\mathrm{cut},\gamma}$. The blue band represents the statistical errors in $E_{\mathrm{cut},\gamma}$.

that the TeV emission seen by HAWC and *Fermi*-LAT is of hadronic origin and that a possible leptonic emission is subdominant. For a detailed study of the leptonic scenario using *FERMI*-LAT data, we refer to Ref. [62] (see also [63,64] on this topic). See [65] for ultra-high-energy gamma-ray emission as a generic feature of pulsars reported by the HAWC collaboration.

B. Neutrino event rate from the eHWC J1825-134 source

In this section we estimate the neutrino flux from the HAWC source as described in Sec. III. We have fixed the normalization and the size of the source to its best-fit values. The spectral index has been also fixed to the best-fit value $\alpha_\gamma = 2.12$. The energy of the cutoff, instead, has been varied within the statistical errors. The results are reported in the right panel of Fig. 3. We report in Table II, the number of atmospheric neutrino events N_{atm} and the number of source events N_{src}, above the following neutrino energy threshold: $E_\nu^{\mathrm{thr}} > 1$, 10, 30 and 100 TeV, for 10 years running time of the KM3NeT detector. Note that since we are considering an effective area optimized for energies above 1 TeV, we chose 1 TeV as the lower energy threshold. The other values are reported to show the number of events in case of analyses optimized for higher energies. As it is clear from the table, the signal events are always significantly above the background as long as the energy threshold is below 10 TeV. If we consider an energy threshold of about 30 TeV the signal events are reduced to 1.8, in case of $E_{\mathrm{cut},\gamma} = 61$ TeV, while to 1.3 and 2.3 in case of $E_{\mathrm{cut},\gamma}$ within the statistical error band. For an even higher energy threshold of about 100 TeV, the number of expected signal events is below one.

Moreover, we want to comment on the statistical error of α_γ in the calculation of the neutrino events. We obtain 1.3 above 1 TeV for the maximum value of α_γ and 1.26 for its minimum value, considering $E_{\mathrm{cut},\gamma} = 49$ TeV, while 1.45 and 1.38 for $E_{\mathrm{cut},\gamma} = 61$ TeV and finally 1.57 and 1.49 for $E_{\mathrm{cut},\gamma} = 73$ TeV. As can be seen from these numbers, considering a value of α_γ different with respect to the best-fit, the events change of about 4% respect to the first column reported in Table II. For this reason, we will show

TABLE II. Number of events for the atmospheric background, N_{atm}, and for the source, N_{src}, above a certain neutrino energy E_ν for ten years of running of the KM3NeT detector. In the "best-fit" case $E_{\mathrm{cut},\gamma}$ is fixed to the best-fit value, while in the "statistical" case the cut off energy is varied within the statistical errors provided in Table I.

Events in 10 yrs	$E_\nu^{\mathrm{thr}} > 1$ TeV	>10 TeV	>30 TeV	>100 TeV
N_{atm}	10.0	1.1	0.2	0.02
N_{src} *(best-fit)*	14.2	6.3	1.8	0.1
N_{src} *(statistical)*	12.8; 15.3	5.2; 7.2	1.3; 2.3	0.06; 0.2

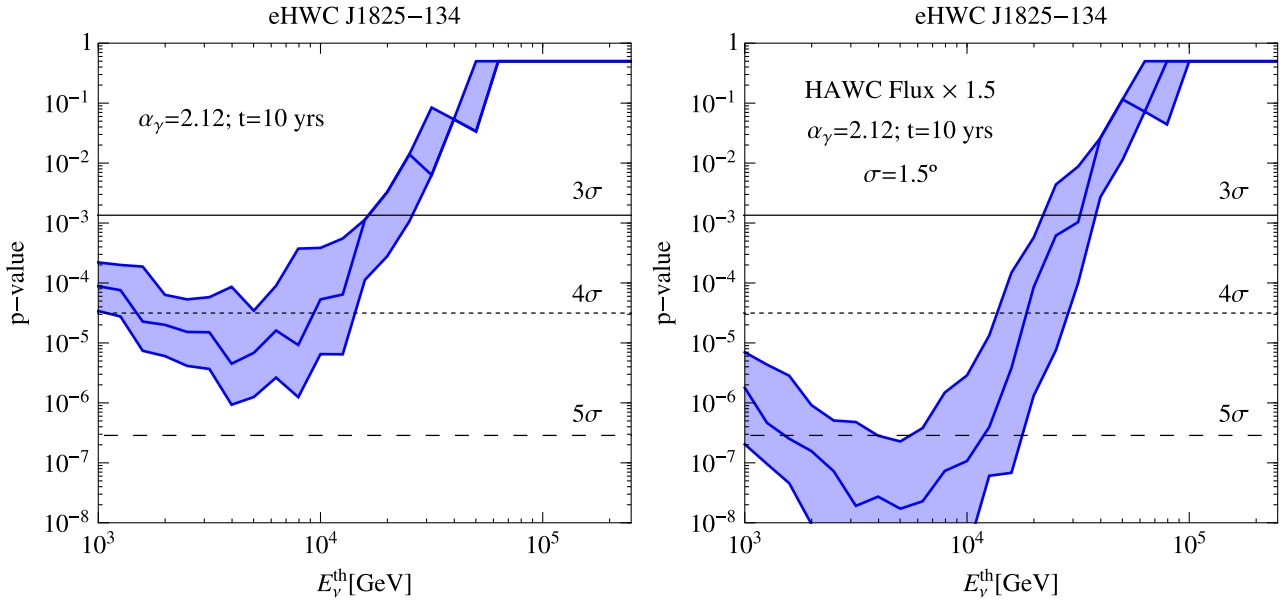

FIG. 4. p-value for the best-fit value of α_γ and different values of $E_{\rm cut,\gamma}$ for 10 years of running of the KM3NeT detector. The blue band represents the statistical errors in $E_{\rm cut,\gamma}$. In the left panel, we have considered the normalization best-fit as provided by the HAWC collaboration and the extension of the source is fixed to 0.53°, while in the right panel we have considered the HAWC flux multiplied by 1.5 and an opening angle of 1.5°.

in the following, only the results considering α_γ as fixed to the best-fit value.

We have estimated the statistical significance as reported in Ref. [66] and as described in Refs. [36,37]. We report in the left panel of Fig. 4 the results for the p-value as a function of the energy threshold for 10 years of running time of the KM3NeT detector and $\alpha \sim 2.12$. We can see that for an energy threshold of the order of $E_\nu^{\rm thr} \lesssim 10$ TeV we have a minimum p-value. We can see that in 10 years of running of KM3NeT the significance is well above 3σ as long as the energy threshold is less than about 10 TeV.

Even if both HESS sources are 100% of leptonic origin, the remaining diffuse emission seen by HAWC would still be detected by KM3NeT at about the 3σ level for a threshold in neutrino energy of the order of 20 TeV, where the contribution of the two HESS sources is negligible ($\lesssim$15%). However at lower energies, the minimum p-value will be reduced from $\gtrsim 4\sigma$ (see left panel of Fig. 4) to between 2σ and 3σ. In this respect, a detection of this source at KM3NeT will also be important to establish the nature of the emission.

C. Neutrino event rate from the eHWC J1825-134 extended region

Here, we estimate the neutrino event rate in KM3NeT considering the region of the 1.5° radius indicated as a dashed green circle in Fig. 1. We take the *Fermi*-LAT flux as reference, and so we repeat the calculation as in Sec. III by multiplying the HAWC gamma-ray flux by a factor of 1.5. In order to account for the more extended region, we set $\sigma_{\rm eff} = 1.5°$, and moreover $\epsilon_\theta = 1$ (i.e., we do not assume a Gaussian morphology). The number of atmospheric neutrino events and of source events from the extended region are reported in Table III for 10 years running time of the KM3NeT detector and for different neutrino energy threshold. Note that in Table II and in Table III, the signal-to-noise ratio is better in the >100 TeV

TABLE III. Number of events considering the eHWC J1825-134 extended region. $N_{\rm atm}^{\rm ext}$ refers to the atmospheric background, while $N_{\rm src}^{\rm ext}$ to the source, considering different neutrino energy threshold and for ten years of running of the KM3NeT detector. In the "best-fit" case $E_{\rm cut,\gamma}$ is fixed to the best-fit value, while in the "statistical" case the cut off energy is varied within the statistical errors provided in Table I.

Events in 10 yrs	$E_\nu^{\rm thr} > 1$ TeV	>10 TeV	>30 TeV	>100 TeV
$N_{\rm atm}^{\rm ext}$	30.2	3.2	0.6	0.07
$N_{\rm src}^{\rm ext}$ *(best-fit)*	29.5	13.1	3.7	0.2
$N_{\rm src}^{\rm ext}$ *(statistical)*	26.8; 31.8	10.9; 14.9	2.7; 4.7	0.1; 0.4

bin, but the chance of detection is worse than the larger than 10 TeV bin, due to the very low expected statistics.

The results are shown in the right panel of Fig. 4, where the p-value is plotted. In this case, the statistical significance reaches 5σ in the case of 10 years running time and for an energy threshold of the order of about 10 TeV. In this scenario, even if the emission from the two HESS sources is leptonic, KM3NeT would detect the emission at the level of roughly 4σ for a neutrino energy threshold of about 20 TeV.

D. Neutrino event rate from the HAWC J1825-134 source

Recently, it has been reported that the eHWC J1825-134 source has been resolved into three different sources by the HAWC collaboration [67]. In particular, HAWC J1825-138 and HAWC J1826-128 are extended, and HAWC 1825-134 is consistent with a point source. The two extended sources are compatible in position with the sources HESS J1825-137 and HESS J1826-130, detected by HESS. They are likely associated with two energetic pulsars, PSR J1826-1334 and PSR J1826-1256, respectively. We want to stress, as stated before, that the gamma-ray pulsar emission can be ascribed to leptonic as well as hadronic models. Under the assumption that the emission from pulsars is leptonic, we have calculated in the following the neutrino expected from the HAWC J1825-134 source. We found that above 1 TeV 0.2 events are expected and 0.025 background events. Since the number of neutrino events is small, we have fixed for this case the neutrino energy threshold to 1 TeV and we have considered the p-value as a function of the running time of the KM3NeT detector, that we report in Fig. 5. As can be seen from the figure, the p-value reaches 3σ when the running time of the KM3NeT detector is around 20 years.

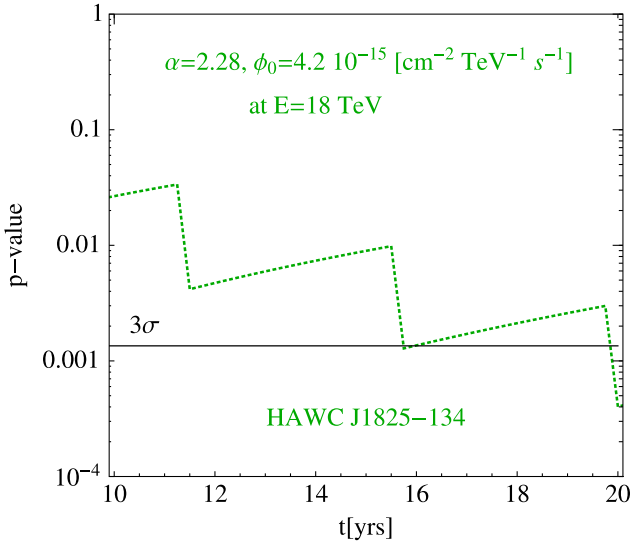

FIG. 5. p-value as a function of the running time of the KM3NeT detector for the source HAWC J1825-134. The values of the parameters α and ϕ_0 has been fixed to the best-fit values. No cut-off has been considered in the analysis and the source is assumed to be pointlike.

E. Comparison with previous studies

This source was previously studied in Ref. [68], where an effective area with six building blocks for the KM3NeT detector was considered along with an angular opening of 0.9° radius. The authors found that the neutrino flux from the source 2HWC J1825-134 is above the sensitivity for 10 years running of the KM3NeT detector within a wide range of energies.

Comparing with the KM3NeT study for point sources with a spectrum $dN/dE \propto E^{-2}$, we can see that a source with the same normalization of eHWC J1825-134 is above the sensitivity for a 5σ detection at the KM3NeT detector within three years of running time [45]. Considering the cut off energy, a discovery at more than 4σ could be reached in about 10 years.

This source is below the sensitivity of the ANTARES data reported in Ref. [45] for point sources with a spectrum $dN/dE \propto E^{-2}$ (see also Ref. [69] for the ANTARES seven years of data for a source with $E_{\mathrm{cut},\nu} < 100$ TeV).

For the possibility of discovering this source at the IceCube detector, we refer to Ref. [27], where an analysis over seven years of tracks and cascade events was considered for specific value of the cut off energy $E_{\mathrm{cut},\nu} =$ 100 TeV and 1 PeV. From what reported, the cascade channels represent the most promising way to discover this source at the IceCube detector.

V. CONCLUSIONS

In this paper, we have analyzed the source eHWC J1825-134. In particular, using updated information on the spectrum provided by HAWC, we calculated the number of events expected at the KM3NeT detector for 10 years running time.

Different potential PeVatron sources have been analyzed in the literature, considering the IceCube detector. Among those, MGRO J1908 + 06 was predicted to be one of the most promising source to be detected at IceCube [33–37]. Since the source eHWC J1825-134 is among the brightest in the multi-TeV domain in the southern sky, we have estimated its discovery potential at the KM3NeT detector assuming that its emission is hadronic. Will eHWC J1825-134 be the first PeVatron source detected by the KM3NeT detector?

Note that also the BAIKAL-GVD detector [70,71] in Baikal Lake will have the discovery potential for this source similar to the KM3NeT detector. We didn't carry out an estimation for this detector since its effective area for muon tracks is currently not public.

Also the key difference of KM3 detectors in water respect to the IceCube detector is a much better angular resolution of cascade events, which is about 2 degrees [45] instead of about 10 degrees. Since the HAWC source eHWC J1825-134 has degree scale itself, additional signal from this source will come from the cascade channel in water KM3 detectors, besides the tracks events. This should increase additionally the sensitivity of KM3 detectors to this source.

We want to add that a possible combined analysis between tracks and cascades, see for example the analysis done by the ANTARES detector in Ref. [69], or between data coming from different KM3 detectors could improve the sensitivity to this source.

ACKNOWLEDGMENTS

This project has received funding from the European Union's Horizon 2020 research and innovation program under the Marie Skłodowska-Curie Grant Agreement No. 843418 (nuHEDGE). S. G. acknowledges support from Agence Nationale de la Recherche (Grant No. ANR- 17-CE31-0014) and from the Observatory of Paris (Action Fédératrice CTA).

[1] S. Gabici, C. Evoli, D. Gaggero, P. Lipari, P. Mertsch, E. Orlando, A. Strong, and A. Vittino, The origin of Galactic cosmic rays: Challenges to the standard paradigm, Int. J. Mod. Phys. D **28**, 1930022 (2019).

[2] M. Kachelriess and D. V. Semikoz, Cosmic ray models, Prog. Part. Nucl. Phys. **109**, 103710 (2019).

[3] A. M. Hillas, The cosmic-ray knee and ensuing spectrum seen as a consequence of Bell's self-magnetized SNR shock acceleration process, J. Phys. Conf. Ser. **47**, 168 (2006).

[4] G. Giacinti, M. Kachelrieß, and D. V. Semikoz, Explaining the spectra of cosmic ray groups above the knee by escape from the Galaxy, Phys. Rev. D **90**, 041302 (2014).

[5] A. Bell, K. Schure, B. Reville, and G. Giacinti, Cosmic ray acceleration and escape from supernova remnants, Mon. Not. R. Astron. Soc. **431**, 415 (2013).

[6] L. O'C. Drury, Galactic cosmic rays—Theory and Interpretation, Proc. Sci., ICRC2017 (**2018**) 1081 [arXiv:1708.08858].

[7] A. Abramowski *et al.* (H.E.S.S. Collaboration), Acceleration of petaelectronvolt protons in the Galactic Centre, Nature (London) **531**, 476 (2016).

[8] S. Gabici and F. A. Aharonian, Searching for galactic cosmic ray pevatrons with multi-TeV gamma rays and neutrinos, Astrophys. J. **665**, L131 (2007).

[9] R. Abbasi *et al.* (IceCube Collaboration), The IceCube high-energy starting event sample: Description and flux characterization with 7.5 years of data, arXiv:2011.03545 [Phys. Rev. D (to be published)].

[10] M. Ahlers, Neutrino Sources from a Multi-Messenger Perspective, EPJ Web Conf. **209**, 01013 (2019).

[11] A. M. Taylor, S. Gabici, and F. Aharonian, Galactic halo origin of the neutrinos detected by IceCube, Phys. Rev. D **89**, 103003 (2014).

[12] A. Neronov, M. Kachelrieß, and D. V. Semikoz, Multimessenger gamma-ray counterpart of the IceCube neutrino signal, Phys. Rev. D **98**, 023004 (2018).

[13] A. Neronov and D. V. Semikoz, Evidence the Galactic contribution to the IceCube astrophysical neutrino flux, Astropart. Phys. **75**, 60 (2016).

[14] A. Neronov, D. V. Semikoz, and C. Tchernin, PeV neutrinos from interactions of cosmic rays with the interstellar medium in the Galaxy, Phys. Rev. D **89**, 103002 (2014).

[15] A. Palladino and F. Vissani, Extragalactic plus Galactic model for IceCube neutrino events, Astrophys. J. **826**, 185 (2016).

[16] G. Pagliaroli, C. Evoli, and F. L. Villante, Expectations for high energy diffuse galactic neutrinos for different cosmic ray distributions, J. Cosmol. Astropart. Phys. 11 (2016) 004.

[17] D. Gaggero, D. Grasso, A. Marinelli, A. Urbano, and M. Valli, The gamma-ray and neutrino sky: A consistent picture of *Fermi*-LAT, Milagro, and IceCube results, Astrophys. J. **815**, L25 (2015).

[18] M. Ahlers, Y. Bai, V. Barger, and R. Lu, Galactic neutrinos in the TeV to PeV range, Phys. Rev. D **93**, 013009 (2016).

[19] M. G. Aartsen *et al.* (IceCube Collaboration), Neutrino emission from the direction of the blazar TXS 0506 + 056 prior to the IceCube-170922A alert, Science **361**, 147 (2018).

[20] P. Padovani, P. Giommi, E. Resconi, T. Glauch, B. Arsioli, N. Sahakyan, and M. Huber, Dissecting the region around IceCube-170922A: The blazar TXS 0506 + 056 as the first cosmic neutrino source, Mon. Not. R. Astron. Soc. **480**, 192 (2018).

[21] S. Gao, A. Fedynitch, W. Winter, and M. Pohl, Modelling the coincident observation of a high-energy neutrino and a bright blazar flare, Nat. Astron. **3**, 88 (2019).

[22] A. Keivani *et al.*, A multimessenger picture of the flaring blazar TXS 0506 + 056: Implications for high-energy neutrino emission and cosmic ray acceleration, Astrophys. J. **864**, 84 (2018).

[23] K. Murase, F. Oikonomou, and M. Petropoulou, Blazar flares as an origin of high-energy cosmic neutrinos? Astrophys. J. **865**, 124 (2018).

[24] A. U. Abeysekara *et al.*, The 2HWC HAWC observatory gamma ray catalog, Astrophys. J. **843**, 40 (2017).

[25] K. A. Malone, A survey of the highest-energy astrophysical sources with the HAWC Observatory, Ph. D. thesis, Penn State U., 2018, https://etda.libraries.psu.edu/catalog/15923kam686.

[26] A. U. Abeysekara *et al.* (HAWC Collaboration), A New Population of Ultra-High-Energy Gamma-Ray Sources Detected by HAWC, Phys. Rev. Lett. **124**, 021102 (2020).
[27] M. G. Aartsen *et al.*, Search for sources of astrophysical neutrinos using seven years of IceCube cascade events, Astrophys. J. **886**, 12 (2019).
[28] M. G. Aartsen *et al.* (IceCube Collaboration), Search for PeV gamma-ray emission from the Southern hemisphere with 5 years of data from the IceCube Observatory, Astrophys. J. **891**, 9 (2020).
[29] M. D. Kistler and J. F. Beacom, Guaranteed and prospective Galactic TeV neutrino sources, Phys. Rev. D **74**, 063007 (2006).
[30] F. Vissani, F. Aharonian, and N. Sahakyan, On the detectability of high-energy galactic neutrino sources, Astropart. Phys. **34**, 778 (2011).
[31] F. Vissani and F. Aharonian, Galactic sources of high-energy neutrinos: Highlights, Nucl. Instrum. Methods Phys. Res., Sect. A **692**, 5 (2012).
[32] S. Gabici, A. M. Taylor, R. J. White, S. Casanova, and F. A. Aharonian, The diffuse neutrino flux from the inner Galaxy: Constraints from very high energy gamma-ray observations, Astropart. Phys. **30**, 180 (2008).
[33] F. Halzen, A. Kappes, and A. O'Murchadha, Prospects for identifying the sources of the Galactic cosmic rays with IceCube, Phys. Rev. D **78**, 063004 (2008).
[34] A. Kappes, F. Halzen, and A. O. Murchadha, Prospects of identifying the sources of the galactic cosmic rays with IceCube, Nucl. Instrum. Methods Phys. Res., Sect. A **602**, 117 (2009).
[35] M. Gonzalez-Garcia, F. Halzen, and S. Mohapatra, Identifying Galactic PeVatrons with neutrinos, Astropart. Phys. **31**, 437 (2009).
[36] M. C. Gonzalez-Garcia, F. Halzen, and V. Niro, Reevaluation of the prospect of observing neutrinos from galactic sources in the light of recent results in gamma ray and neutrino astronomy, Astropart. Phys. **57–58**, 39 (2014).
[37] F. Halzen, A. Kheirandish, and V. Niro, Prospects for detecting galactic sources of cosmic neutrinos with IceCube: An update, Astropart. Phys. **86**, 46 (2017).
[38] A. Kheirandish and J. Wood (IceCube and HAWC Collaborations), IceCube search for galactic neutrino sources based on HAWC observations of the Galactic Plane, Proc. Sci., ICRC2019 (**2020**) 932 [arXiv:1908.08546].
[39] A. U. Abeysekara *et al.*, Observation of the crab nebula with the HAWC gamma-ray observatory, Astrophys. J. **843**, 39 (2017).
[40] A. U. Abeysekara *et al.* (HAWC Collaboration), Measurement of the crab nebula at the highest energies with HAWC, Astrophys. J. **881**, 134 (2019).
[41] F. Aharonian *et al.* (H.E.S.S. Collaboration), Energy dependent gamma-ray morphology in the Pulsar wind nebula HESS J1825-137, Astron. Astrophys. **460**, 365 (2006).
[42] H. Abdalla *et al.* (HESS Collaboration), Particle transport within the pulsar wind nebula HESS J1825-137, Astron. Astrophys. **621**, A116 (2019).
[43] O. E. Angüner, S. Casanova, I. Oya, F. Aharonian, P. Bordas, and A. Ziegler (H. E. S. S. Collaboration), Very high energy emission from the hard spectrum sources HESS J1641-463, HESS J1741-302 and HESS J1826-130, Proc. Sci., ICRC2017 (**2018**) 686 [arXiv:1708.04844].
[44] F. L. Villante and F. Vissani, How precisely neutrino emission from supernova remnants can be constrained by gamma ray observations? Phys. Rev. D **78**, 103007 (2008).
[45] S. Adrian-Martinez *et al.* (KM3Net Collaboration), Letter of intent for KM3NeT 2.0, J. Phys. G **43**, 084001 (2016).
[46] A. Kappes, J. Hinton, C. Stegmann, and F. A. Aharonian, Potential neutrino signals from galactic gamma-ray sources, Astrophys. J. **656**, 870 (2007).
[47] D. Alexandreas, D. Berley, S. Biller, G. Dion, J. Goodman *et al.*, Point source search techniques in ultrahigh-energy gamma-ray astronomy, Nucl. Instrum. Methods Phys. Res., Sect. A **328**, 570 (1993).
[48] S. Kelner, F. A. Aharonian, and V. Bugayov, Energy spectra of gamma-rays, electrons and neutrinos produced at proton-proton interactions in the very high energy regime, Phys. Rev. D **74**, 034018 (2006).
[49] M. Honda, T. Kajita, K. Kasahara, and S. Midorikawa, Improvement of low energy atmospheric neutrino flux calculation using the JAM nuclear interaction model, Phys. Rev. D **83**, 123001 (2011).
[50] L. Volkova, Energy spectra and angular distributions of atmospheric neutrinos, Sov. J. Nucl. Phys. **31**, 784 (1980), https://ui.adsabs.harvard.edu/abs/1980SvJNP..31..784V/abstract.
[51] P. Gondolo, G. Ingelman, and M. Thunman, Charm production and high-energy atmospheric muon and neutrino fluxes, Astropart. Phys. **5**, 309 (1996).
[52] P. Bruel, T. H. Burnett, S. W. Digel, G. Johannesson, N. Omodei, and M. Wood (*Fermi*-LAT Collaboration), *Fermi*-LAT improved Pass 8 event selection, in *8th International Fermi Symposium: Celebrating 10 Year of Fermi Baltimore, Maryland, USA* (2018).
[53] A. Neronov and D. Semikoz, Galactic diffuse gamma-ray emission at TeV energy, Astron. Astrophys. **633**, A94 (2020).
[54] B. M. Gaensler and P. O. Slane, The evolution and structure of pulsar wind nebulae, Annu. Rev. Astron. Astrophys. **44**, 17 (2006).
[55] W. Bednarek, Neutrinos from the pulsar wind nebulae, Astron. Astrophys. **407**, 1 (2003).
[56] I. D. Palma, D. Guetta, and E. Amato, Revised predictions of neutrino fluxes from pulsar wind nebulae, Astrophys. J. **836**, 159 (2017).
[57] M. Lemoine, K. Kotera, and J. Pétri, On ultra-high energy cosmic ray acceleration at the termination shock of young pulsar winds, J. Cosmol. Astropart. Phys. 07 (2015) 016.
[58] G. Principe, A. M. W. Mitchell, S. Caroff, J. A. Hinton, R. D. Parsons, and S. Funk, Energy dependent morphology of the pulsar wind nebula HESS J1825-137 with *Fermi*-LAT, Astron. Astrophys. **640**, A76 (2020).
[59] S. Abdollahi *et al.* (*Fermi*-LAT Collaboration), *Fermi* large area telescope fourth source catalog, Astrophys. J. Suppl. **247**, 33 (2020).

[60] A. Neronov and D. Malyshev, Hard spectrum of cosmic rays in the disks of milky way and large magellanic cloud, arXiv:1505.07601.

[61] R. Yang, F. Aharonian, and C. Evoli, Radial distribution of the diffuse γ-ray emissivity in the Galactic disk, Phys. Rev. D **93**, 123007 (2016).

[62] M. Di Mauro, S. Manconi, M. Negro, and F. Donato, Investigating γ-ray halos around three HAWC bright sources in *Fermi*-LAT data, arXiv:2012.05932.

[63] A. Albert *et al.*, Probing the sea of cosmic rays by measuring gamma-ray emission from passive giant molecular clouds, arXiv:2101.07895.

[64] T. Sudoh, T. Linden, and D. Hooper, The highest energy HAWC sources are leptonic and powered by pulsars, arXiv:2101.11026.

[65] A. Albert *et al.* (HAWC Collaboration), Evidence that ultra-high-energy gamma rays are a universal feature near powerful pulsars, Astrophys. J. Lett. **911**, L27 (2021).

[66] ATLAS, CMS, LHC Higgs Combination Group Collaboration, Procedure for the LHC Higgs boson search combination in summer 2011.

[67] A. Albert *et al.*, Evidence of 200 TeV photons from HAWC J1825-134, Astrophys. J. Lett. **907**, L30 (2021).

[68] L. Ambrogi, S. Celli, and F. Aharonian, On the potential of Cherenkov telescope arrays and KM3 neutrino telescopes for the detection of extended sources, Astropart. Phys. **100**, 69 (2018).

[69] A. Albert *et al.* (ANTARES Collaboration), First all-flavor neutrino pointlike source search with the ANTARES neutrino telescope, Phys. Rev. D **96**, 082001 (2017).

[70] A. D. Avrorin *et al.* (Baikal-GVD Collaboration), Neutrino telescope in Lake Baikal: Present and future, Proc. Sci., ICRC2019 (**2020**) 1011 [arXiv:1908.05427].

[71] A. D. Avrorin *et al.* (Baikal-GVD Collaboration), Search for cascade events with Baikal-GVD, Proc. Sci., ICRC2019 (**2021**) 873 [arXiv:1908.05430].